Renewable Energy 70 (2014) 62–77

Contents lists available at ScienceDirect

Renewable Energy

journal homepage: www.elsevier.com/locate/renene

Blind Test 2 calculations for two in-line model wind turbines where the downstream turbine operates at various rotational speeds

Fabio Pierella, Per-Åge Krogstad, Lars Sætran*

Dep. Energy and Process Engineering, Norwegian University of Science and Technology NTNU, Trondheim 7491, Norway

ARTICLE INFO

Article history:
Received 30 September 2013
Accepted 7 March 2014
Available online 4 April 2014

Keywords:
Wind turbine modeling
Experiment
Simulation comparison
Blind Test 2

ABSTRACT

In this paper we report on the results of the Blind Test 2 workshop, organized by Norcowe and Nowitech in Trondheim, Norway in October 2012. This workshop was arranged in order to find out how well wind turbine simulation models perform when applied to two turbines operating in line. Modelers with a suitable code were given boundary conditions of a wind tunnel test performed in the large wind tunnel facility at the Department of Energy and Process Engineering, at NTNU Trondheim, where two almost identical model turbines with a diameter of about 0.9 ~ m had been tested under various operating conditions. A detailed geometry specification of the models could be downloaded and the modelers were invited to submit the calculation without knowing the experimental results in advance.

Nine different contributions from eight institutions were received, representing a wide range of simulation models, such as a LES coupled with an actuator line rotor model, RANS using an actuator disc, U-RANS models applied to fully resolved turbine model geometries, as well as a vortex panel method. The comparison showed a larger than expected scatter on the performance calculation of the upstream turbine (±20%), and an even higher uncertainty for the downstream turbine, especially at operating conditions close to the runaway point. The modelers were requested to document the wake development downstream of the second turbine, the development behind the first turbine had been the challenge for a previous blind test (see Krogstad and Eriksen [17]).

Mean flow calculations reported at $X = 1$D downstream of the second turbine showed that the models which fully resolved boundary layers on the rotor surface performed best. Including the tower and the hub in the simulation improved the accuracy of the predictions and is essential in capturing the important asymmetries that develop in the wake. These turbine details strongly influence the development near the center of the wake, but are often omitted in simulations in order to incorporate simplifying symmetry conditions in the calculations. Further from the rotor, at $X = 4$D, the LES simulations coupled to actuator line rotor models performed well and were able to capture the main features of the mean and turbulent flows, while RANS models using actuator disc models showed limitations especially in predicting correctly the turbulent kinetic energy.

1. Introduction

In the last 20 years, as the knowledge on wind turbine aerodynamics and the availability of computational power increased, numerical models are becoming more and more complex. The driving force behind model optimization is achieving a good compromise between the physics in the model and the computational effort, which is a direct function of the grid points needed to resolve the case. Most of the early models relied heavily on assumptions and shortcuts which needed to be calibrated against experimental data, see for example the work from Jensen [14], Ainslie [2] or Crespo et al. [6]. More recently, full CFD models have been employed in order to resolve the flow in greater detail. Correctly modeling the rotor remains the key issue to address when accurate predictions are needed. Two options are basically available: either fully resolving the blade geometry with its boundary layers or modeling the rotor as a force field. The first option is computationally demanding, see e.g. the work from Zahle et al. [38], but allows the model to predict complex effects, like 3D flow on the rotor surface or unsteady airfoil behavior. In less complicated cases, it is more efficient to calculate the force field exerted by the rotor using 2D airfoil data. In the actuator disc approach by

* Corresponding author. Tel.: +47 73593716.
E-mail addresses: fabio.pierella@ntnu.no (F. Pierella), lars.saetran@ntnu.no (L. Sætran).

http://dx.doi.org/10.1016/j.renene.2014.03.034
0960-1481/

Sørensen et al. [33] the turbine is represented as a disc with a variable thrust and torque distribution, while in the actuator line model, see e.g. Troldborg [35], the turbine blades are represented as rotating point forces. Independently of the rotor resolution technique, the flow field simulation is usually carried out by a N–S solver using a LES, RANS or U-RANS approach. All of the numerical contributions to this workshop used a CFD approach; on the other hand, simple analytical models are still the standard for industrial applications. It is by comparisons with well executed physical experiments, see for example Snel et al. [31] or Simms et al. [29], that more advanced computational models can be validated and prove their reliability also for the industry.

Turbine simulation models have a decisive role in wind farm planning. Ideally, the model predictions should be verified against full scale experiments before the farm is built. But since this is not possible, the model predictions need to be verified either against similar full scale configurations where data is available, against relevant wind tunnel experiments, or the prediction model must have otherwise proven its reliability so that the results are known to be trustworthy.

In full scale experiments used for comparison, the inflow conditions are usually not well defined and may contain a fair amount of uncertainty, and the limited amount of data available often makes a comparison difficult, see Vermeer et al. [36] and Krogstad and Eriksen [17].

In wind tunnel experiments, the boundary conditions are more easily controllable, which makes them more suitable for benchmarking purposes. However, full scale key factors like atmospheric turbulence levels, thermal stratification are usually not reproduced, see for example the experiments from Maeda et al. [20]. In most tests, experimental airfoil data are not available for the model Reynolds number, which complicates the interpretation and evaluation of the experimental results, see e.g. Smith [30] or Chamorro and Porté-Agel [4].

Even in a well planned wind tunnel experiment, scaling issues must be correctly handled if a consistent comparison between model and full scale is needed. While matching the tip speed ratio (λ or TSR) of a full scale turbine is not difficult, a complete local Reynold similarity is impossible to achieve. A typical tip Reynolds number of a full scale turbine Re_c^{tip}, based on the relative velocity of the tip and the blade tip chord, is of the order of 10^6. For a wind tunnel model this number varies between 10^4 and 10^5, see e.g. Alfredsson and Dahlberg [3], Smith [30] and Medici and Alfredsson [22]. However, since the scope of the current experiments was not to simulate a full scale case but rather to provide high quality data for the benchmarking of wind turbine simulation models, the scaling issues are considered of secondary importance. Scaling issues will be further discussed in Section 2.1.

Previous blind test challenges have shown that numerically reproducing the behavior of a single wind turbine in uniform flow, despite being the most basic of the test cases, is a complicated task. One example where the current state of the art was examined is the 2011 Blind Test 1 (BT1) workshop, which was organized in Bergen, Norway, see Krogstad and Eriksen [17,16]. The geometry of a model turbine with a rotor diameter of $D = 0.894$ m was distributed to interested scientists and participants were asked to predict the turbine performance and the wake development downstream of the turbines. The numerical predictions showed wide scatter and the agreement with the experimental results was found to depend on the numerical model complexity as well as the skills of the operator. For example, among Reynolds averaged computations on fully resolved rotors, the modeler using the least number of points achieved the best agreement with the experimental data. This is probably due to a wiser choice of the grid point distribution.

Fig. 1. Wind tunnel setup.

In general the predictions of the wake mean velocities were in good agreement with the model measurements, and the maximum deviation on the power output at design condition was only about ±15%. On the other hand, the turbulent kinetic energy was on average underestimated by one order of magnitude, and in extreme cases up to three orders of magnitude. In the NREL Unsteady Aerodynamics Experiment, described by Simms et al. [29], the calculation of the performance and wake flow of a full scale rotor was addressed, and similar scatters among the models and deviations from the experimental results were observed.

In 2012 a follow up of BT1 was organized using two similar turbines and a selection of the results will be reported in this paper. The purpose of the Blind Test 2 challenge (BT2), organized in Trondheim, Norway, was to validate the accuracy and reliability of current wind turbine simulation models in the case of two turbines arranged in-line. The downstream separation between the turbines was $S = 3D$. This was judged to be a considerably more complicated flow configuration than in BT1, and is highly relevant in order to optimize wind farm layouts and to correctly assess the return of an investment. Again researchers with a suitable numerical code were invited to try to reproduce the experimental data of performance and wake development when only given the geometrical details of the setup. Hence, much of the challenge lies in choosing the best turbulence model, setting up the optimum numerical flow description and choosing the best model parameters in order to optimize their results. A major effort was made in order to provide high quality and reproducible experimental data and to give to the modelers precise boundary conditions to implement in their calculations.

2. Test case

The model turbines in this study were designed in 2008, for the specific purpose to be used as test cases. This is the reason for many of the design compromises involved, as discussed in Krogstad and Eriksen [17]. Fig. 1 shows the two turbines used in the present blind test located in the wind tunnel. T_1 is the upstream turbine, while T_2 is the downstream one: both turbines were rotating in counterclockwise direction when observed from upstream. The two turbines have the same blade geometry, but slightly different hub size, which leads to somewhat different rotor diameters: $D_1 = 0.894$ m while $D_2 = 0.944$ m.

The experiments were carried out in the large closed-loop wind tunnel facility at NTNU. The wind tunnel has a rectangular test

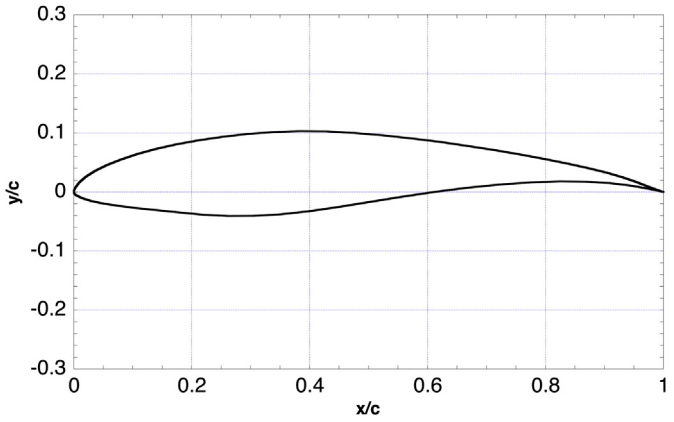

Fig. 2. Airfoil S826.

section, whose dimensions at the inlet are $W = 2.72$ m and $H = 1.80$ m. The test section is $L = 11.15$ m long, and the roof height was adjusted in order to produce zero pressure gradient in the whole test section at the reference velocity used in the tests when the tunnel was empty. The reference velocity was set to $U_{ref} = 10$ m/s. At this velocity the turbulence intensity is TI = 0.3% at the inlet. The boundary layer thickness at the second turbine position was measured to be 0.25D. An invitation document by Pierella et al. [23] contains more complete technical details. A detailed description of the wind tunnel is also present in Krogstad and Adaramola [15], Adaramola and Krogstad [1] and Krogstad and Eriksen [17].

The upstream turbine T_1 was positioned 2D from the test section inlet. It was verified that this location is sufficiently far downstream for the operation of the turbines not to affect the uniformity of the inlet velocity profile. The downstream turbine T_2 was positioned $S = 3$D downstream from the upstream turbine, and both turbines had the same hub height, $H^{hub} = 0.817$ m, see Fig. 3. Both turbines were horizontally centered in the wind tunnel, and were alternately positioned on a high accuracy, six component aerodynamic balance in order to allow the thrust on the rotor to be measured. The thrust of the tower and nacelle was measured and subtracted from the thrust of the turbine, to yield the thrust of the rotor. Each turbine was fitted with a torque transducer and a speed of rotation sensor on the shaft mounted directly behind the rotor. The power generated by both turbines could be measured simultaneously. In the wake, mean and turbulent velocities were measured using hot wire anemometry. The measurement techniques applied were the same as used in BT1, see Krogstad and Eriksen [17] for complete details. The aforementioned invitation document for the Blind Test 2 workshop included all the geometrical details of the turbines, which were made available to the modelers also under form of 3D CAD files.

The rather short separation between the turbines, forced by test section length constraints, introduced some challenges for the modelers who could not accurately model the vortex system downstream of the turbines. This is necessary in order to produce good near wake predictions and therefore correct inlet conditions for T_2. In fact, the results from Blind Test 1 by Krogstad and Eriksen [17] show that at $X = 3$D from the upstream turbine the flow is dominated by distinct near wake features, such as a very thin shear layer and a quasi-top-hat mean streamwise velocity profile, where the helical vortex system is still stable.

2.1. Scaling

Wind tunnel experiments present scaling issues that limit the comparison with full scale turbines. The tip speed ratio similarity is usually easy to achieve. The turbines used in this study were designed for a reference velocity of 10 m/s, and to have an optimum performance at $\lambda = 6$, or approximately 1200 rpm. At this condition, the boundary layers on the blades of T_2 have been verified to be attached. The same proof is not available for T_1, but since the blades are identical for both turbines it appears reasonable to assume that this also is the case for T_1. At lower than optimum tip speed ratio, the streamwise momentum for the stalled rotor sections is relatively small, and the centrifugal force induces a spanwise flow which is deviated toward the trailing edge of the blade by the Coriolis force. This significantly delays stall and alters the 2D characteristics of the airfoil, see Hansen [13]. Due to the high rotational velocity, this effect is likely to be more pronounced in wind tunnel tests than in full scale turbines.

The tip local Reynolds number is $Re_c^{tip} \approx 10^5$ for the upstream turbine at maximum performance, while for a full scale wind turbine this parameter is at least one order of magnitude higher.

To make this difference as small as possible, the blade chord of the model turbines were designed to be about 3 times larger than what would normally be used for such a rotor. This implies a higher local Reynolds number, which reduces the possibility of laminar separation and enhances the similarity with full scale experiments, but also implies a rather low lift coefficient of the blade sections at the design condition, see also the discussion in Krogstad and Eriksen [17]. However, as Grant et al. [11] and Vermeer et al. [36] suggest, the limitation can be neglected if the characteristics of the airfoil are known and if the blade tip lift coefficient is similar to

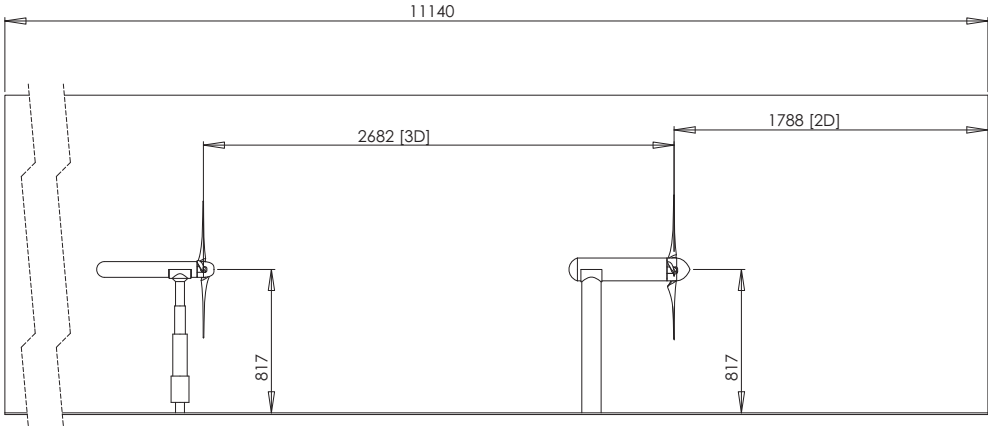

Fig. 3. Wind Tunnel setup, plan. Dimensions in [mm]

the full scale value, which is verified at least for the upstream turbine in the current experiments (compare the experimental values from Sarmast [26] for $Re = 10^5$ and the high Reynolds values from Somers [32]). For the downstream turbine, the high amount of turbulence produced in the flow by the upstream rotor should make the airfoil behavior less sensitive to Reynolds number effects.

The wake generated by the tower is also a function of the flow conditions. In the wind tunnel experiments, the Reynolds number based on the diameter of the largest of the cylinders of T_2 tower was $Re^{\mathrm{T}} \approx 10^5$, yielding a drag coefficient of $C_{\mathrm{D}} \approx 1$. For a full scale turbine, where $Re^{\mathrm{T}} \approx 10^7$, the drag coefficient would be less than half of that, i.e. $C_{\mathrm{D}} \approx 0.4$ (see e.g. Delany and Sørensen [7]). Moreover, in a full scale turbine the ratio between the tower and the rotor diameters would be of the order of 0.05, while in the current experiment it was twice as high. For these reasons, we expect the wake behind a full-scale turbine tower to be less wide than in the current experiments.

In full scale wind tunnel experiments, like the NREL UAE experiments by Simms et al. [29], the local Reynolds is at least $Re_{\mathrm{c}} \approx 10^6$. At that Reynolds number, numerical models which fully resolve the rotor surface would need a much larger number of grid points in order to correctly resolve the boundary layer, leading to a higher computational cost. On the other hand, models which use a force field to simulate the rotor would not experience a dramatic increase in calculation effort. These models would probably perform best at high Reynolds numbers, where the airfoil characteristics will be less Reynolds number sensitive. At low Reynolds numbers the performance may in fact be very sensitive to laminar separations. As for the methods using RANS turbulence models, such as the $k-\varepsilon$ model, these methods are also expected to perform best at high Reynolds numbers. In LES computations of free shear flows, the number of cells required to resolve the flow is proportional to Reynolds number, which increases the ratio between the energy containing length scales and the inertial subrange length scale, but the model accuracy is not affected provided that the correct filter size is chosen, see for example Pope [24].

For a discussion on blockage effects on the experimental data please see the results from Blind Test 1 in Krogstad and Eriksen [17]. It is worth mentioning that it is common practice not to correct for blockage effects when providing experimental data for Blind Tests, since the modelers can easily take into account the effect of the walls by including them in the simulations as no-slip surfaces.

2.2. Airfoil characteristics

The blades use the NREL S826 airfoil along the entire span. The profile was designed to have high lift coefficients, low sensitivity to roughness, and docile stall characteristics, suitable for the tip of low solidity blades as described by Tangler and Somers [34]. The stall is controlled by a so-called separation ramp, a steep slope which confines the initial separation to a zone close to the trailing edge. In Fig. 2 the airfoil section is shown. A complete description of the airfoil, together with high Reynolds lift and drag characteristics, is given by Somers [32].

Low Reynolds experiments from Sarmast [26] show that the airfoil, if operated below $Re^{\mathrm{crit}} \leq 10^5$, is subject to hysteresis connected with the onset of laminar separation bubble near the leading edge, affecting the linear part of the lift curve. At these Reynolds numbers the airfoil also suffers from a strong post-stall hysteresis.

Compressibility can represent an issue on small wind turbines, as reported by Wood [37]. For the most severe tip speed, found at the runaway point, the upstream rotor tip Mach number is $M^{tip} = 0.35$ and the corresponding angle of attack is $\alpha = 1^\circ$. Therefore no serious compressibility effects are expected for most of the operational range. Further references about the blade structural characteristics and design can be found in Krogstad and Eriksen [17] and Krogstad and Lund [18].

Table 1
Simulation parameters. AD = actuator disc, AL = actuator line, FR = Fully resolved, VP = Vortex Panel, N/A = not applicable, RANS = Reynolds Averaged Navier–Stokes, LES = large eddy simulation.

Contributor	Simulation tool	Rotor model	Flow model	Airfoil data
Acona	ANSYS Fluent	FR	RANS $k-\omega$ SST	N/A
CMR	Music	AD	RANS $k-\varepsilon$	Xfoil
deVaal	ANSYS Fluent	AD	RANS $k-\varepsilon$	Q^{3}uick
DTU-KTH	EllipSys3D/FLEX5	AL	LES	Q^{3}uick
GexCon AS	CMR-Wind	AD	RANS $k-\varepsilon$	Xfoil
Leonardi	OpenFOAM	AL	LES	High Re Exp. [32]
Meventus	OpenFOAM	AL [5]	LES	Xfoil
Uzol	Aerosim	VP	Free vortex wake	N/A

2.3. Required output

The modelers were asked to provide predictions for performance and thrust coefficients, and for wake mean and turbulent velocities for three test cases. The wind tunnel reference velocity was set to $U_{\mathrm{ref}} = (10 \pm 0.1)$ m/s for all cases. In all the setups, the upstream turbine, T_1, was rotating at peak efficiency, or $\lambda_1 = 6$. The downstream turbine, T_2, positioned at $S = 3$D, was running at three different tip speed ratios, one close to optimum efficiency ($\lambda_2 \approx 4$ when operating in the wake of T_1 and using U_{ref} in the definition of λ_2). For the next setting T_2 was operated close to the runaway condition and for the least case T_2 was operated in the stall region at low λ_2.

- **Setup A**: $\lambda_1 = 6$, $\lambda_2 = 4$ (Compulsory)
- **Setup B**: $\lambda_1 = 6$, $\lambda_2 = 7$ (Optional high speed case)
- **Setup C**: $\lambda_1 = 6$, $\lambda_2 = 2.5$ (Optional low speed case)

For all cases the first part of the output was the estimated thrust and power coefficients for the upstream and downstream turbines. These are defined as:

$$C_{\mathrm{P}} = 2P/\left(\rho U_{\mathrm{ref}}^3 A\right) \tag{1}$$

$$C_{\mathrm{T}} = 2T/\left(\rho U_{\mathrm{ref}}^3 A\right) \tag{2}$$

where A is the rotor disk area using the actual rotor diameters, D_1 and D_2. The second part of the output consisted of the non-dimensional streamwise mean velocity, $U^* = U/U_{\mathrm{ref}}$, and the normalized streamwise Reynolds stress, $(\mathrm{u}'^*)^2 = \langle \mathrm{u}'\mathrm{u}' \rangle / U_{\mathrm{ref}}^2$ along a horizontal and vertical diagonal through the center of the wake at three different downstream distances from T_2, $X = [1\mathrm{D}, 2.5\mathrm{D}, 4\mathrm{D}]$. ($\langle \bullet \rangle$ denotes time averaged quantities.) The distance was normalized using a nominal rotor diameter of $D = 0.9$ m.

2.4. Method descriptions

Data was received from 8 institutions, who contributed one simulation each, except GexCon who submitted two datasets. Most of them predicted the flows for all three setups.

The participants were asked to submit a method description in order to document the features of their models and document that their results were grid independent. The main characteristics of the models are summarized in table 1. Here follows a brief description of each of them.

2.4.1. Acona flow technology

Manger from Acona Technology was the only participant who fully resolved the entire turbine structures, including the boundary layers on the blades and tower. He also included the wind tunnel walls, thus reproducing the whole test case as it was measured. The turbines blades were finely meshed in a thin sliding mesh block rotating with respect to the main stationary grid, where the turbine structure and the wind tunnel were also finely resolved. The total number of cells was $30 \cdot 10^6$. The simulation was carried out using the *Fluent v. 14.0* software package, with an incompressible solver and a $k-\omega$ SST turbulence closure model. The method also performed quite well in the first Blind Test, again because the modeler included the hub, the nacelle and the walls in the simulation.

The results from Manger will be labeled **Acona**.

2.4.2. CMR Instrumentation

The simulations were performed by Hallanger and Sand using an in-house CFD code called *Music*. The code was developed at CMR, and uses a standard steady state $k-\varepsilon$ model for turbulence closure with the coefficients proposed by Launder and Spalding [19].

The discretized equations are solved on a co-located grid using the SIMPLE algorithm from Ferziger and Perić [9]. The rotors were modeled by an actuator disc with rotation, where the 2D airfoil data were estimated using *Xfoil* (see Drela [8]). A sub-grid turbulence model is added, in order to represent the additional turbulence generation by the wind turbine, adapted from models for flow in large rod bundles by Sha and Launder [28]. The total number of grid points for the case was $3.9 \cdot 10^5$. The walls were included in the simulations, while the towers of the turbines were not modeled. The hubs were taken into account as a flow resistance, but the axial extent of the nacelles was not represented.

The results from Hallanger and Sand will be labeled **CMR**.

2.4.3. De Vaal — NTNU Marintek

De Vaal also performed his calculations using *Fluent v. 14.0*, where a finite volume discretization of the incompressible N–S was implemented. The test case was run on an axisymmetric grid, where the turbine actuator disc was included via a BEM model. The 2D airfoil data were calculated via the *Q*^{3}*uick* software implemented by García [10], and used the same airfoil dataset as the **DTU-KTH** contributors. The grid was composed of 508×236 cells in the streamwise and radial directions, respectively, and axial symmetry was assumed. 80 of the radial cells were used to resolve the rotor span. The tower and the nacelle were not simulated by De Vaal, while the wind tunnel walls were taken into account as no-slip surfaces. The turbulence closure model was the Reynolds Stress model (RSM), as implemented in the *Fluent* package.

The simulations from De Vaal will be marked **DeVaal**.

2.4.4. DTU and Linné Flow Center, KTH

Mikkelsen of DTU and Sarmast from KTH performed a large eddy simulation using the *EllipSys3D* code developed by Risø and DTU. The computational domain is a regular Cartesian grid of the same size as the wind tunnel, meshed using a total of 43 million grid points. The turbine rotor was modeled using the actuator line concept (see e.g. Troldborg [35]), and discretized by 43 points along each blade, on which the loads were calculated. The boundary conditions were constant inflow velocity and convective outflow, and the wind tunnel walls were included as no-slip surfaces. The wind tunnel turbulence was modeled introducing synthetic turbulent fluctuations at $X = 1.5$D upstream of the first wind turbine, following the method by Mann [21]. The 2D airfoil data were obtained from the in-house developed viscous–inviscid interactive code *Q*^{3}*uick* from García [10]. The sub-grid scale viscosity is modeled using a vorticity-based mixed scale model, see Sagaut [25].

The simulations from Mikkelsen and Sarmast will be labeled **DTU-KTH**.

2.4.5. GexCon

GexCon was the only modeler who submitted two simulations. The GexCon group, represented by Khalil and Sælen used an in-house software package called *FLACSeWind*, a transient CFD solver which uses the standard $k-\varepsilon$ turbulence model. The computational domain was similar to the wind tunnel dimensions, but without the increase in tunnel height to compensate for the growth of side wall boundary layers. The rotor was represented as an actuator disk, and the turbine tower and nacelle were not included in the simulation. The 2D airfoil data were obtained by Hansen via *XFoil*, see Drela [8]. The model used for the two simulations is the same, with the difference that in what is marked as **GexCon-sim1**, the walls, floor and roof were modeled as no-slip boundaries, while in **GexCon-sim2** there were no walls.

2.4.6. University of Puerto Rico

Leonardi and Martinez Tossas, from the University of Puerto Rico, used OpenFOAM to perform a LES simulation with a standard Smagorinsky sub-grid scale model ($C_S = 0.1$), where the turbine rotors were simulated as actuator lines. The walls, roof and floors were included in the simulation as no-slip surfaces, while the towers and the nacelles of the turbines were not simulated. High Reynolds number airfoil data from Somers [32] were used as input for the simulations, and the *AirfoilPrep* tool from NREL [12] was used to correct the airfoil data for rotational effects.

The results from University of Puerto Rico will be labeled **Leonardi**.

2.4.7. Meventus

The simulation from Meventus were performed by Lund and Bhutoria, who resolved the flow via a LES simulation with a standard Smagorinsky sub-grid scale model ($C_S = 0.1$). The rotor was simulated via an actuator line model, which is included in the SOWFA package [5] developed by NREL for OpenFOAM. The 2D airfoil data were again calculated using *XFoil* with a $N_{crit} = 3$ (see Krogstad and Lund [18] for further details). While the test section walls were included in the simulation as no-slip boundaries, the effect of the nacelle and of the tower was not modeled. The total number of cells in the simulation was $4.3 \cdot 10^5$.

The results from Meventus will be labeled **Meventus**.

2.4.8. METU

The results from METU, the Middle East Technical University, were produced by Uzol and Sezer Uzol. The authors used the free-wake code *AeroSIM+*, a 3D unsteady free-wake vortex panel method. For the turbines, the blades are discretized using quadrilateral panel elements and vortex ring elements are placed within each element. During an unsteady run, at each time instant, the influence coefficients of surface and wake panels are calculated using the induced velocity values from each vortex segment on the collocation points by means of the Biot-Savart law. Then the blades are moved and a new solution is calculated for the next time step. No tower or hub were modeled, while the boundaries of the wind tunnel were treated as no-slip surfaces.

The results from METU will be labeled **Uzol**.

2.4.9. Numerical and experimental uncertainties

The modelers were asked to provide proof of grid independency of their solution, even though not all of the modelers could provide sufficient proof. DTU-KTH showed that the calculations performed

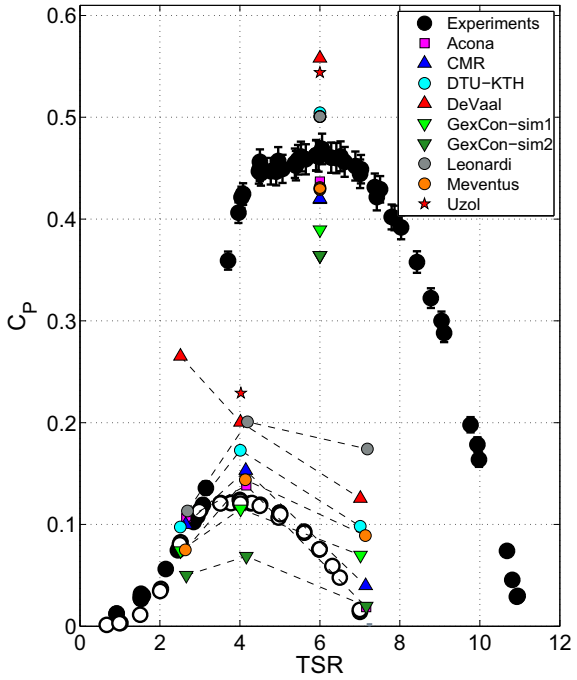

Fig. 4. Experimental C_P of T_1 (filled circles) and T_2 (empty circles) vs. simulations. The upstream turbine was running at fixed $\lambda_1 = 6$ while the downstream turbine was run at $\lambda_2 = 4$, 7 and 2.5 for setups A,B and C.

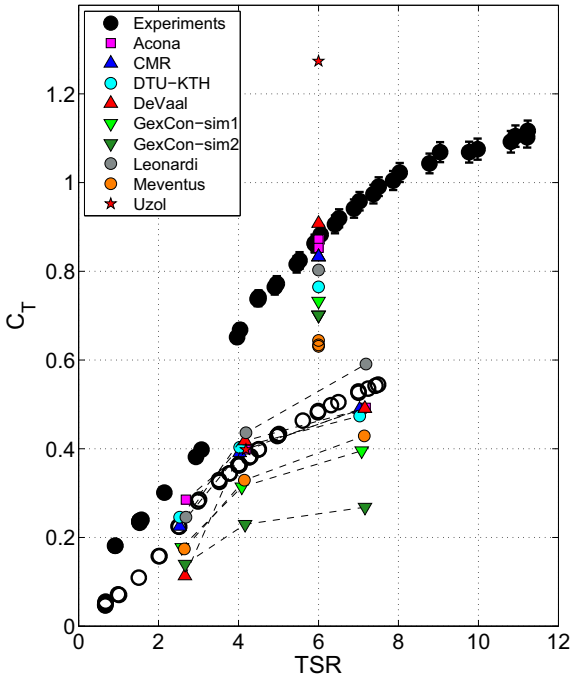

Fig. 5. Experimental C_T of T_1 (filled circles) and T_2 (empty circles) vs. simulations. The upstream turbine was running at fixed $\lambda_1 = 6$ while the downstream turbine was run at $\lambda_2 = 2.5$, 4 and 7.

on a very fine grid with 2.4 times the number of cells used in the grid for the submitted results, led to a change in the calculated maximum C_P of 2%. The grid independency presented by CMR and Leonardi showed a similar discrepancy between the C_P calculated on the finest grid and on the final grid used for calculations. Acona and GexCon did not present any grid independency data. The LES from Meventus was performed on a coarser mesh than DTU-KTH. The grid independency of the solution was verified on a mesh with 4.5 times as many cells as in the grid used for the submitted calculations. A maximum variation of 3% on the power and thrust coefficient of the two turbines was observed. The results from the free wake code from Uzol were sampled for a too short time, hence the wiggles visible in the mean wake profiles, see for example Fig. 6.

The experimental uncertainty on the thrust and performance measurements was calculated with a 95% confidence interval, which, for T_1 means ±3% on the peak efficiency and ±2% on the thrust coefficient at peak performance. The uncertainty on the mean velocity and streamwise normal stress was also calculated with a 95% confidence interval. The uncertainty on the mean velocity was largest outside of the wake, where the fluid velocity is highest and the velocity sensitivity of the hot wire is lowest, while the uncertainty on the turbulent stresses peaked in the wake shear layer. The uncertainty in the measurements depend on the case settings and measurement positions and are therefore included in all the figures to be presented in the next section.

3. Results

In the following plots, the marker symbols used are indicative of the rotor modeling techniques: a square means that the rotor was fully resolved, a triangle is used when the rotor was modeled as an actuator disc and a circle when modeled as an actuator line. The vortex panel method of Uzol is indicated by a five pointed star.

3.1. Power and thrust prediction

Figs. 4 and 5 show the power and thrust calculations for the nine contributions. The numerical values are also summarized in Table 2 for reference. The calculations for the upstream turbine showed a surprisingly large scatter (±20%) in the power coefficient compared to the value measured for the turbine at the design operating point of $\lambda_1 = 6$. This may be partly due to the turbine operating in a Reynolds number sensitive region and partly because the aerodynamic properties of the airfoil used were not specified by the organizers. Experiments performed at DTU, Denmark, on the S826 airfoil by Sarmast [26] highlighted the onset of hysteresis at moderate angles of attack ($5^\circ < \alpha < 10^\circ$) on the linear part of the lift coefficient curve for $Re^{crit} \leq 10^5$, probably triggered by laminar separation bubbles, which is compatible with the operating condition of the inner 1/4 of the blade of the upstream turbine rotor at $\lambda_1 = 6$.

However, when the same airfoil data sets were used in different BEM models, as in the case of De Vaal and DTU-KTH, the predicted values varied significantly, suggesting that the predictions depend just as much on how the data was used. In this case De Vaal used an actuator disk model while DTU-KTH used the actuator line model. Judging from the predicted power coefficient, the more complicated actuator line method appears to give better estimates than the actuator disk model, giving an offset from the experimental value of only 7% versus 19% for De Vaal. Acona's predictions, the only one which fully resolved the whole rotor surface and the turbine structure, performed quite well, underestimating the experimental value by only 7%.

Fig. 5 shows a similar scatter for the thrust coefficients. The free vortex method of Uzol gave an unrealistically high thrust for T_1, while all the other models either matched or underpredicted the rotor thrust compared to the measurements. However, the scatter between them was 30% of the experimental value. Acona's results again gave the best agreement. The actuator disc predictions from

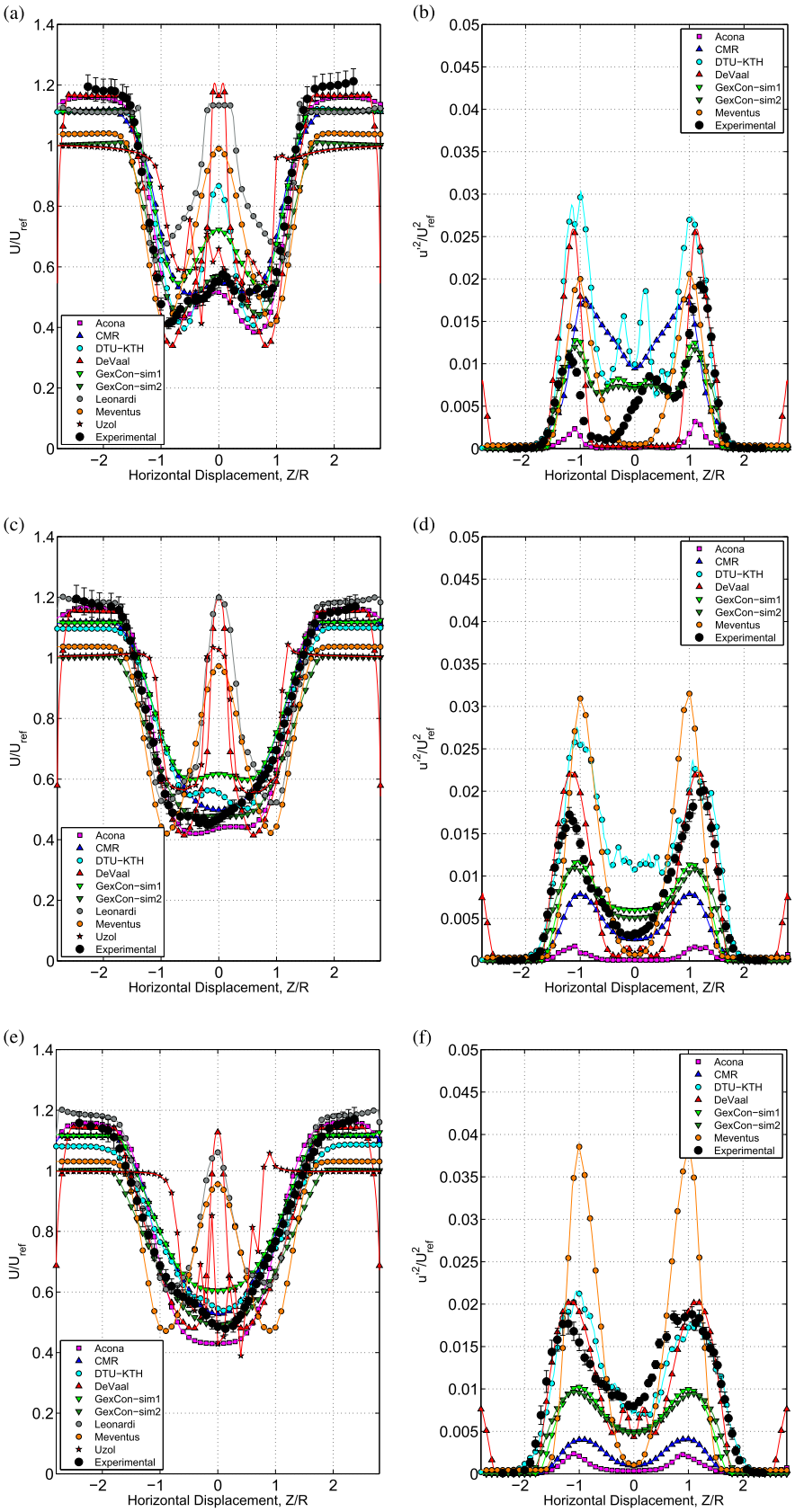

Fig. 6. Setup A: wake development. The upstream turbine was running at $\lambda_1 = 6$ while the downstream turbine at $\lambda_2 = 4$. (a): U/U_{ref} at $X = 1$D, Horizontal. (b): u'^2/U^2_{ref} at $X = 1$D, Horizontal. (c): U/U_{ref} at $X = 2.5$D, Horizontal. (d): u'^2/U^2_{ref} at $X = 2.5$D, Horizontal. (e): U/U_{ref} at $X = 4$D, Horizontal. (f): u'^2/U^2_{ref} at $X = 4$D, Horizontal.

Table 2
Summary of the numerical results for power and thrust. The upstream turbine was running at fixed $\lambda_1 = 6$ while the downstream turbine was run at $\lambda_2 = 4$, 7 and 2.5 for setups A, B and C.

	T_1		T_2 Set. A		T_2 Set. B		T_2 Set. C	
	C_P	C_T	C_P	C_T	C_P	C_T	C_P	C_T
Experimental	0.469	0.883	0.121	0.363	0.014	0.526	0.082	0.224
Acona	0.437	0.872	0.138	0.398	0.019	0.492	0.106	0.285
CMR	0.420	0.833	0.153	0.391	0.040	0.489	0.100	0.225
DTU-KTH	0.504	0.765	0.173	0.403	0.098	0.474	0.098	0.246
DeVaal	0.558	0.908	0.200	0.418	0.126	0.491	0.265	0.113
GexCon-sim1	0.389	0.733	0.115	0.314	0.070	0.395	0.074	0.177
GexCon-sim2	0.364	0.701	0.069	0.229	0.020	0.268	0.050	0.140
Leonardi	0.501	0.803	0.201	0.436	0.174	0.591	0.113	0.246
Meventus	0.431	0.644	0.144	0.329	0.089	0.429	0.075	0.174
Uzol	0.544	1.274	0.229	0.398	–	–	–	–

De Vaal and CMR matched closely the thrust of the rotor. However, they did not agree about the power prediction, suggesting that the airfoil performance data they used are very different. All the actuator line methods had a tendency to underpredict the thrust, in the same way as was observed in Blind Test 1. The GexCon-2 simulation, which did not include the walls, show lower power and thrust values than the one with walls (GexCon-sim1), indicating a significant effect of the solid blockage on the rotor performance. The power coefficients predicted for T_2 (Fig. 4) show more scatter than for T_1. The downstream turbine had its peak efficiency at $\lambda_2 = 4$ (Setup A), while the figure shows that in Setup B, at $\lambda_2 = 7$, the turbine was close to the runaway point. Since the incoming velocity profile that T_2 sees is not homogeneous, it is difficult to estimate the operating conditions of the rotor sections in Setup B. Fig. 4b of Krogstad and Eriksen [17] shows that the wake at $X = 3$D behind a single turbine working at $\lambda = 6$, which is the inflow condition for the downstream turbine of this study, can be approximated by an irregular top-hat profile, with a half-width of 0.5D and a depth of $U/U_{ref} = 0.6$. Fig. 7a, which shows the near wake at $X = 1$D behind T_2 in Setup B, suggests that at this operating condition the inner part of the downstream turbine rotor was feeding momentum into the flow and thus working in a propeller state, while the outer part was extracting energy from the flow, working at a relatively low angle of attack due to the high tangential velocity. At the runaway point, these two components even out. Fig. 8a gives less information about the working state of the rotor in Setup C ($\lambda_2 = 2.5$). A first approximation analysis of the velocity triangles, performed by neglecting the rotor induction and considering a constant inflow velocity profile of 6 m/s, indicates that the blade inner sections were heavily stalled and extracted no energy from the flow, while the outer sections, also working at rather high angles of attack, harvested the necessary power to yield an efficiency of $C_P = 0.08$.

Despite the low incoming velocity and the consequent low local Reynolds number on the T_2 rotor blades, the experimental performance curve had a smooth shape, see Fig. 4. In fact, when turbine T_2 is running alone in the wind tunnel in an undisturbed flow with a free stream velocity lower than 9 m/s (Krogstad and Adaramola [15]) the onset of laminar separation in the inner sections of the rotor generates a sudden drop in the power and thrust curve at λ_2 between 4 and 7. Since no such irregularities were visible in Fig. 4, we can infer that the high turbulence intensity induced by the upstream turbine triggered the transition to turbulent regime before laminar separation occurred.

At $\lambda_2 = 4$, the power coefficient predicted by GexCon-sim1 was quite accurate, matching the experimental results within an accuracy of 5%, while the simulation without the walls (GexCon-sim2) predicted a significantly lower performance, 42% lower than the experimental one. The fully resolved simulation from Acona again performed well, overestimating only marginally the power production. Despite using the same 2D airfoil data, DTU-KTH and De Vaal had again different power results, with the actuator line model being more accurate and predicting an efficiency of $C_P = 0.173$ versus the experimental value of $C_P = 0.121$. This result is remarkable, since a higher thrust prediction for the first turbine means less kinetic energy available to the second turbine, and in this sense the prediction from DTU-KTH should have been higher than the ones from De Vaal. This leads us to think that De Vaal's model overestimated the turbulent diffusion in the wake and hence the velocity deficit recovery rate. The free wake method from Uzol overestimated the downstream turbine power production by about 90%, compared to the 16% error on the upstream turbine efficiency.

For $\lambda_2 = 2.5$ the experimental efficiency of the downstream turbine was measured to be $C_P = 0.082$. The scatter between the BEM methods is on average smaller than for $\lambda_2 = 4$, probably due to a better agreement in the prediction of the deep stall behavior of the airfoil. The fully resolved rotor simulation from Acona overestimated the power production, while GexCon-sim1 and Meventus predictions were more accurate, within ±5% from the experimental value. All the other methods overestimated the power production, except for the GexCon-sim2 which did not include the wind tunnel wall effects.

At $\lambda_2 = 7$ the power production was very close to zero, but most of the methods did not suggest that this is close to the runaway point. Again Acona performed well, together with the actuator disc method from CMR and GexCon-sim2. Acona's good results are not surprising: at this tip speed ratio the inner part of the rotor is working as a propeller, giving birth to strong spanwise flow patterns which methods based on 2D airfoil predictions are not able to catch.

The difference between the two GexCon simulations conveys a clear message on the importance of blockage with respect to wind tunnel operation. In fact the two simulations predicted similar thrust values for the upstream turbine, allowing an equal amount of kinetic energy through the rotor. Therefore, one would expect the same performance also for the downstream turbine, but GexCon-sim2 constantly outputted lower thrust and power values for T_2 than GexCon-sim1 (27% lower in setup A).

Except for the predictions of De Vaal, all the simulations predicted the optimum performance at $\lambda_2 = 4$ while only a few methods found a lower efficiency for $\lambda_2 = 7$ than for $\lambda_2 = 2.5$. DeVaal's method predicted a higher maximum velocity deficit for setup C than for setup A, suggesting an error in the calculation of the angle of attack on the downstream turbine rotor. In fact, at $\lambda_2 = 2.5$, the low tangential velocity of the turbine rotor makes the relative inflow angle very sensitive to the incoming flow velocity magnitude, so errors in predictions of the upstream turbine wake lead to bigger errors in the downstream turbine performance for setup C than for setup A and B. There seems to be no general trend to suggest that the actuator line model is better than an actuator disc model, which means that for performance calculations a more complex model does not necessarily give a better prediction than a less complicated one, exception made for models resolving the detailed flow over the rotor. The incoming flow on the second turbine was not a required output for the current experiments, so it is not always possible to state whether the errors in prediction come mostly from inaccurate calculations on the first or rather on the second turbine rotor.

The T_2 thrust calculations for low tip speed ratio, in Fig. 5, are scattered around the experimental values within ±50%, while the thrust values at high rotational rates are generally underpredicted. The CMR method performs very well throughout the whole tip speed range, being in close agreement with the experiments. At $\lambda = 4$ both GexCon simulations output low estimates, with GexCon-sim2 being 37% off and GexCon-sim1 14% off the experimental value.

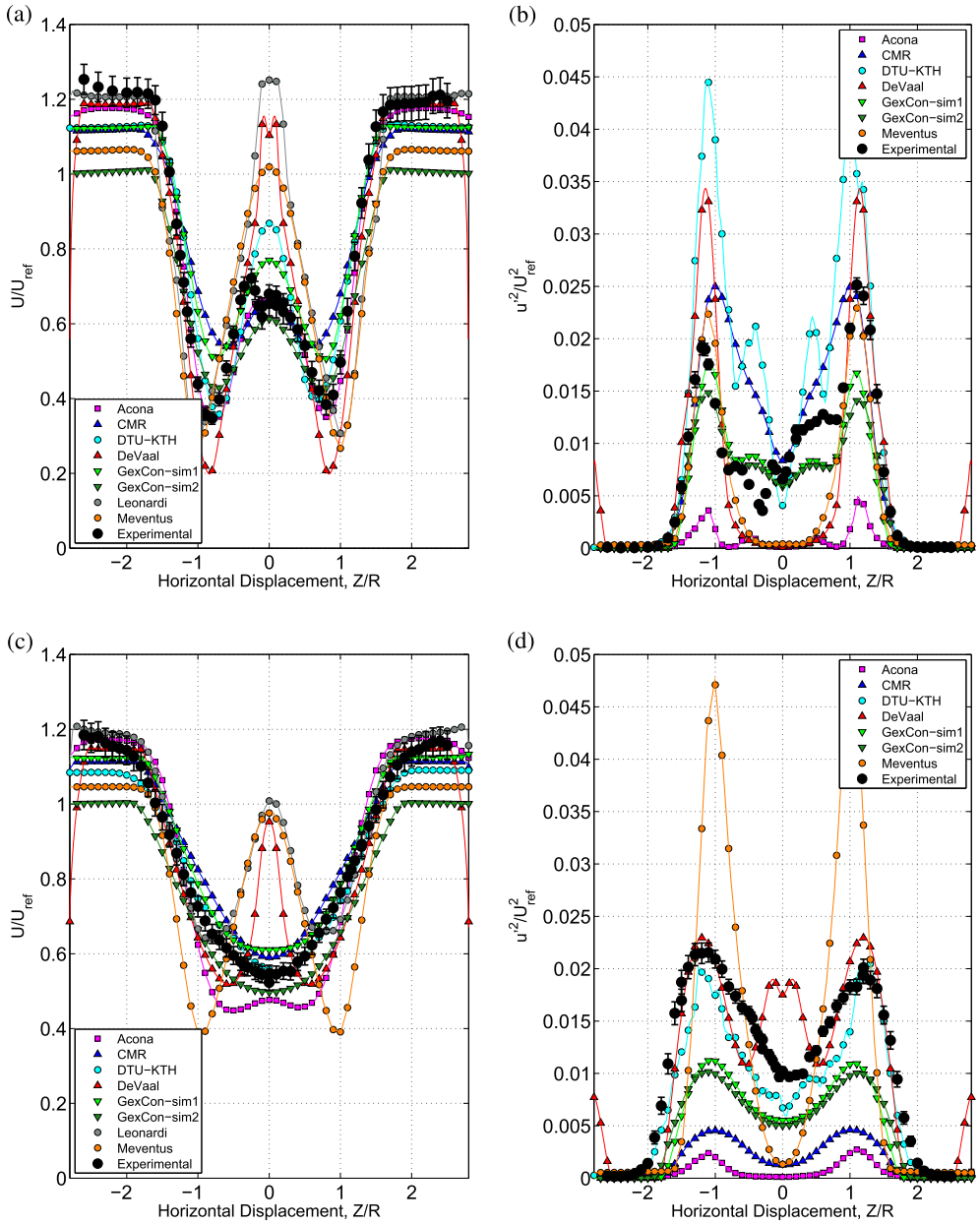

Fig. 7. Wake predictions for the turbine tandem, Setup B. The upstream turbine was running at $\lambda_1 = 6$ while the downstream turbine at $\lambda_2 = 7$. (a): U/U_{ref} at $X = 1$D, Horizontal, Setup B. (b): u'^2/U^2_{ref} at $X = 1$D, Horizontal, Setup B. (c): U/U_{ref} at $X = 4$D, Horizontal, Setup B. (d): u'^2/U^2_{ref} at $X = 4$D, Horizontal, Setup B.

This appears to be a general trend throughout all the setups, and is probably due to inaccurate estimates of the 2D airfoil performance. At $\lambda = 7$ the thrust predicted is lower than the measurements ($C_T = 0.526$) for all the simulations, except for the one by Leonardi, which predicted a $C_T = 0.591$. Leonardi consistently over-predicted the thrust and performance for both turbines, which is probably due to his choice of using the high Reynolds number 2D airfoil data from Somers [32] as an input for the BEM method. Amongst the actuator line methods, the one from DTU-KTH agrees best with the thrust data throughout the analyzed tip speed ratio range, with a maximum error at $\lambda_2 = 7$ of 10%. Again, it is not possible to say whether it is the actuator disc or line method which is the preferred method. Obviously there is a computational benefit of using the simpler actuator disc model due to the lower computational power demand (e.g. the total number of cells used by CMR is $\approx 10^5$ while DTU-KTH used approximately 10^7 cells).

As a general comment, only the Acona model produced high quality predictions under all conditions, while the other models showed high variability and sensitivity to the operating conditions of the turbines.

3.2. Wake prediction

3.2.1. Setup A ($\lambda_1 = 6$, $\lambda_2 = 4$)

The participants were asked to provide velocity and stress profiles along a horizontal and vertical diagonal passing through the axis of rotation for the two turbines. In this way it could be checked if the methods that included more than the rotor blades were able to capture the expected flow asymmetries. We start by presenting the data along the horizontal diagonals.

The experimental mean velocity profile at $X = 1$D (Fig. 6a) was slightly asymmetric, due to the wake generated by the tower. The

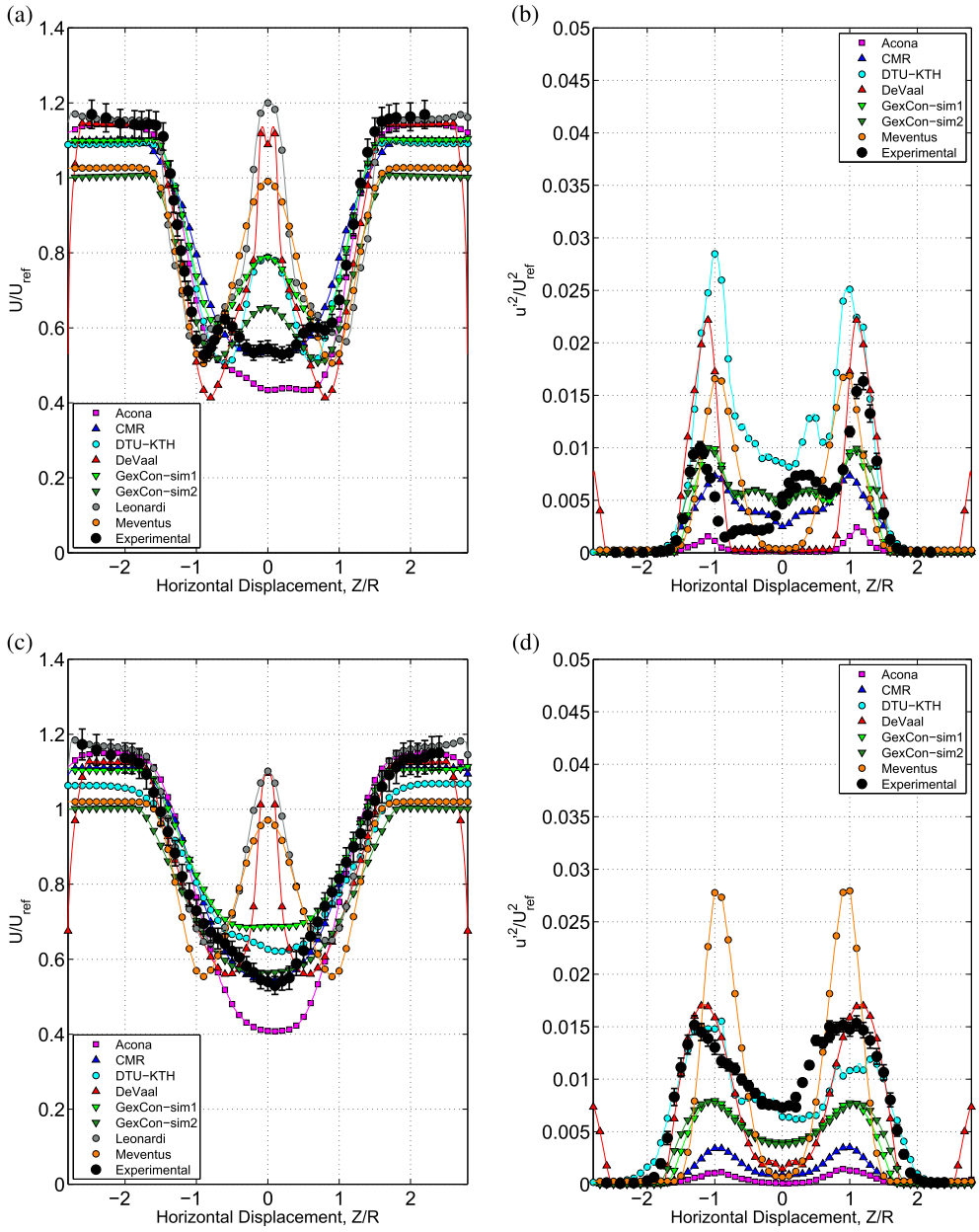

Fig. 8. Wake predictions for the turbine tandem, Setup C. The upstream turbine was running at $\lambda_1 = 6$ while the downstream turbine at $\lambda_2 = 2.5$. (a): U/U_{ref} at $X = 1$D, Horizontal, Setup C. (b): u'^2/U^2_{ref} at $X = 1$D, Horizontal, Setup C. (c): U/U_{ref} at $X = 4$D, Horizontal, Setup C. (d): u'^2/U^2_{ref} at $X = 4$D, Horizontal, Setup C.

velocity outside of the wake was 20% higher than the reference velocity due to the blockage effect of the turbine, which produces an overall drag coefficient of about 1.2. Therefore, the modelers who underestimated the thrust for both turbines, like Meventus, predicted a reduced velocity increase outside of the wake. Furthermore, not including the walls in the simulation also led to a deviation in the prediction of the undisturbed velocity, as the 10% difference between GexCon-1 and GexCon-2 demonstrates.

At the wake centre line, the simulations which included the nacelle (Acona and CMR) performed best, while the others featured a strong velocity overshoot caused by the fluid bypassing the rotor disc through the gap in the centre. Only the Acona model managed to reproduce the asymmetry in the wake maximum velocity deficit measurements, even though not as marked as in the experiments where the difference between the velocity measured at $Z = \pm$R was 10% of the U_{ref}. Experiments by Schümann et al. [27] on a single turbine show that such asymmetries are generated by the advection of the tower wake by the swirling rotor wake. This effect can obviously be caught only by simulations which include the tower in their calculations.

The predictions from Uzol showed a too shallow wake and a not very smooth velocity profile, probably due to a too short sampling time. The width of the turbine wake seemed to be captured reasonably well by most of the models, except by the free wake code from Uzol, which produced a rather narrow wake.

At $X = 2.5$D (Fig. 6c), the turbulent diffusion started to dominate the wake evolution. The velocity deficit was wider and smoother than at the previous station, but still rather asymmetric. Both the velocity deficit and the mean velocity gradient in the shear layer were stronger on the negative than on the positive side of the Z axis. Among the modelers which did not include the presence of the hub and tower, the simulations from Leonardi, Meventus and De Vaal

still featured a high velocity peak at the wake centre line, while the LES from DTU-KTH exhibited a regular and smooth profile. In Fig. 6d it may be clearly seen how the turbulence intensity at $Z = 0$ for the DTU-KTH was at least twice as high as in all other simulations, indicating that the difference in the mean velocity profiles can be explained by a differences in turbulent diffusion predicted by the different models. The simulation by Acona gave a virtually perfect mean velocity predictions in the shear layer, while it calculated a 10% too deep velocity deficit between $Z = 0$ and $Z = R$. CMR's predictions were even better than the ones from Acona for positive Z, but the symmetric velocity profile was less accurate for $Z^{\circ}<^{\circ}0$. The GexCon-1 model predicted quite correct wake width and the velocity decay in the shear layer, but the underestimation in the thrust led to a too shallow velocity deficit.

At $X = 4$D the wake centre line deficit has started to recover, see Fig. 6e. The maximum non-dimensional velocity deficit is 0.49, against 0.46 for the previous measurement station and this time it is positioned on the positive Z axis, having been shifted by the wake rotation. The wake covers almost the whole measurement span and the profile has a nearly Gaussian shape. The method from CMR performed very well across the whole span, while Acona's predictions were too pessimistic especially in the centre of the wake, indicating an underestimation in the turbulent diffusion as confirmed by the low turbulence levels produced at all downstream distances. Both simulations from GexCon had a regular bell shape, but while the one without the walls predicted 20% too low velocities outside of the wake, the one including the walls calculated a 20% too high velocity at the centre line. The LES from Meventus was the model producing the largest deviation from the measurements. It gave too low velocities in the outer part of the wake, too high gradients in the shear layer and a 100% overshoot at the centre line due to the missing nacelle. On the other hand, the LES from Leonardi and the RANS-RSM from De Vaal performed quite well in the outer part of the wake and in the shear layer, but the velocity peak at the centre line was still over 100% too high, again as a consequence of omitting the nacelle. The free wake code from Uzol gave unstable velocity profiles, and markedly overestimated the recovery of the wake, predicting for $X = 4$D a very narrow wake. The LES from DTU-KTH seemed to perform well across the whole span, giving probably the best overall distributions among all the methods.

In Table 3, two relevant wake parameters, the wake width and the centerline velocity, are given for all the setups both for the experiment and the simulations for $X = 4$D. Overall, only two out of nine models predict the wake width within ±5%, but seven out of nine are within ±15%. This indicates that the wake width is satisfactorily captured by most models, except by the free wake model from Uzol and the LES from Meventus. Most of the simulations predict the centerline velocity to within ±15%. However, the results from DeVaal, Leonardi and Meventus are less accurate.

Close to the rotor ($X = 1$D), the experimental streamwise Reynolds stress profile, Fig. 6b, features three distinct peaks, two in the outer wake shear layer and one at the wake centre line, slightly skewed to the positive side of the Z axis. This centre peak comes from the nacelle and the tower wakes. All the models predicted a turbulence intensity of the same order of magnitude as in the measurements, contrarily to what was seen in BT1, where the predictions were orders of magnitude too low. The LES from DTU-KTH produced oscillations in the turbulent stress at this station, especially near the centre, where additional turbulence was generated in the shear layer produced by the centerline velocity overshoot. The simulations from Acona also reproduced two strong peaks in the shear layer, even though the level is much too low. The author of the simulations suggested this may be related to problems in the interpolation of the turbulent kinetic energy at the interface between the revolving rotor mesh and the background grid. However, the method did not predict the peak at the wake centre line observed in the measurements, despite the fact that the computations included the entire model in the simulations. The CMR model predicted mostly too high turbulence intensity, especially on the left half of the rotor span where the turbulent stress was measured to be nearly zero for $Z \approx -0.5$R. This is probably due to an overestimation of the rotor generated turbulence by the applied sub-grid model. The model from Meventus matched very well the right shear layer turbulence peak, but obviously could not reproduce the secondary peak at the centre of the wake due to lack of geometrical details and to the coarse computational grid. It is worth pointing out that the models using a two equation closure for turbulence (Acona, CMR, GexCon) predicted mostly lower turbulence levels than the models which could resolve the Reynolds stress tensor components, especially at higher downstream distances. Those who only predicted the total kinetic energy and not the stress distributions were invited to calculate the normal turbulent stress assuming the isotropic turbulence relation:

$$k \simeq 3u'^2 \Big/ 2. \tag{3}$$

This assumption is probably not very appropriate for the zones of largest mean velocity shear, where the stress tensor has been shown to be highly anisotropic (see. e.g Krogstad and Eriksen [17], Vermeer et al. [36]). Therefore this simplification might have contributed to the negative bias observed for the models using a 2-equation closure.

At the second downstream station, Fig. 6d, turbulent diffusion has made all profiles smoother. The turbulence peaks observed at $Z = \pm R$ are much wider and the peak at $Z = 0$ is no longer visible. It has partly been advected by the rotation away from the horizontal diagonal and partly been smoothed out by turbulent diffusion (cfr. the measurements from Schümann et al. [27]). The Acona model, which produced too low turbulence at the previous downstream distance, is still about one order of magnitude lower than the measurements. The turbulence predicted by the GexCon model is almost unaffected by the distance traveled downstream from the previous position, indicating that the production and dissipation of turbulence are in equilibrium in the model. The calculations from CMR at $Z = \pm R$ are 50% lower than the measurements, but perform very well at the centre line. The LES simulations from DTU-KTH and the RSM from De Vaal predict the correct turbulence levels within 10%, but show little variation from $X = 1$D to $X = 2.5$D. Except for

Table 3
Summary of the results at $X = 4$D on a horizontal diagonal for all setups, see Figs. 6e, 7c and 8c. ΔZ is the normalized distance between the points where $U/U_{mean} = 0.8$. This value has been chosen because it roughly represents the velocity for which the experimental profiles have an inflection point. The U_{CL}/U_{ref} is the centerline non-dimensional velocity at $X = 4$D for all setups. The upstream turbine was running at fixed $\lambda_1 = 6$ while the downstream turbine was run at $\lambda_2 = 4{,}7$ and 2.5 for setups A,B and C.

	Set. A		Set. B		Set. C	
	$\Delta Z_{U/U_{ref}=0.8}$	U_{CL}/U_{ref}	$\Delta Z_{U/U_{ref}=0.8}$	U_{CL}/U_{ref}	$\Delta Z_{U/U_{ref}=0.8}$	U_{CL}/U_{ref}
Experimental	2.30 R	0.49	2.26 R	0.55	2.12 R	0.52
Acona	2.16 R	0.43	2.32 R	0.48	2.10 R	0.41
CMR	2.01 R	0.53	1.88 R	0.59	1.99 R	0.54
DTU-KTH	2.24 R	0.55	2.29 R	0.56	2.06 R	0.63
DeVaal	2.46 R	1.13	2.53 R	0.95	2.39 R	1.10
GexCon-sim1	1.99 R	0.60	2.06 R	0.61	1.86 R	0.69
GexCon-sim2	2.63 R	0.49	2.68 R	0.50	2.51 R	0.56
Leonardi	2.41 R	1.06	2.40 R	1.01	2.36 R	1.10
Meventus	2.71 R	0.96	2.77 R	0.98	2.58 R	0.97
Uzol	1.44 R	0.43	–	–	–	–

Table 4
Summary of the results at $X = 4D$ on a horizontal diagonal for all setups, see Figs. 6f, 7d and 8d. The $(u'^2/U^2_{ref})_{max}$ is the maximum normalized Reynolds stress found on a horizontal diagonal at $X = 4D$, while $(u'^2/U^2_{ref})_{CL}$ is the centerline ($Z = 0$) normalized Reynolds stress on a horizontal diagonal at $X = 4D$. The upstream turbine was running at fixed $\lambda_1 = 6$ while the downstream turbine was run at $\lambda_2 = 4$, 7 and 2.5 for setups A, B and C.

	Set. A		Set. B		Set. C	
	$(u'^2/U^2_{ref})_{max}$	$(u'^2/U^2_{ref})_{CL}$	$(u'^2/U^2_{ref})_{max}$	$(u'^2/U^2_{ref})_{CL}$	$(u'^2/U^2_{ref})_{max}$	$(u'^2/U^2_{ref})_{CL}$
Experimental	1.89e-02	8.07e-03	2.15e-02	1.02e-02	1.53e-02	6.89e-03
Acona	2.38e-03	3.48e-04	2.74e-03	1.21e-04	1.57e-03	9.52e-05
CMR	4.14e-03	9.91e-04	4.63e-03	1.27e-03	3.59e-03	9.28e-04
DTU-KTH	2.16e-02	7.50e-03	2.05e-02	6.68e-03	1.57e-02	6.41e-03
DeVaal	2.03e-02	4.36e-03	2.30e-02	1.75e-02	1.71e-02	1.46e-03
GexCon-sim1	1.02e-02	4.95e-03	1.13e-02	5.51e-03	7.95e-03	3.98e-03
GexCon-sim2	9.64e-03	4.75e-03	1.02e-02	5.01e-03	7.85e-03	3.79e-03
Leonardi	–	–	–	–	–	–
Meventus	3.88e-02	1.02e-03	4.88e-02	1.31e-03	2.80e-02	6.62e-04
Uzol	–	–	–	–	–	–

the centre region this also applies to the experiments. The Meventus LES on the other hand shows a strong increase in turbulence level and very little diffusion, which seems to some extent unphysical.

At $X = 4D$ the turbulent diffusion has transferred a considerably amount of turbulence across to the wake centre (see Fig. 6f and Table 4). All the 2-equations models are now predicting too low turbulence intensities, which seems to confirm that such turbulence models are too dissipative to correctly represent a complicated anisotropic turbulent flow. The actuator line LES from DTU-KTH and RSM from De Vaal agree quite well with the experimental data all the way across the wake. They employed the same airfoil data for their predictions, but totally different descriptions of the turbulent transport process.

Selecting a winner amongst the presented model is not an easy task. The different models lead to different levels of precision at the various measurement stations downstream of the turbines. The fully resolved rotor calculations from Acona performs very well close to the rotor, but suffers from low turbulence level predictions in the wake. The LES from DTU-KTH is more accurate far from the turbines, but is less accurate at the station closest to the turbine, mainly because the hubs and the towers of the models are not included and representing the rotor by a force field will not produce very accurate velocity fields in the immediate vicinity of the model. The 2D actuator disc/CFD model from De Vaal, despite being computationally very cheap, shows very good turbulence and mean velocity wake predictions far from the rotor. But its axisymmetry assumption is intrinsically unable to reproduce the asymmetry structure in the wake.

3.2.2. Setup B ($\lambda_1 = 6$, $\lambda_2 = 7$)

In Setup B the downstream turbine was running close to the runaway condition. In Fig. 7a the high velocity at the rotor centre line indicates that the inner part of the rotor was working as a propeller, feeding energy into the wake. The outer part of the rotor is operating at low angles of attack and extracts energy from the flow. This working condition was chosen because of the strong three-dimensionality expected across the blades. The uneven pressure distribution induces a spanwise flow along the blade, which needs to be correctly modeled in order to get a correct wake velocity field. In this sense, Acona's and Uzol's methods have an advantage, since they are the only case definitions that directly model the blade surface. Unfortunately, Uzol did not submit any results for setup B and C. An extra complication is constituted by the fact that the outer part of the wake is rotating in the opposite direction of the central part, producing another strong shear layer inside the wake. At $X = 1D$, Acona's simulation closely matched the measured mean velocity wake profile. CMR managed to reproduce the velocity deficit near the wake centre line, but the strong deficit near the blade tips was not captured. This was surprising since C_T for T_2 was well predicted. GexCon-sim2 reproduced the velocity inside the rotor wake quite closely, but predicted 16% too low velocity outside of the wake, due to the absence of the walls. All the models predicted the wake width with acceptable accuracy.

Moving downstream to $X = 4D$ (Fig. 7c) the experimental profile is seen to be smooth and Gaussian, having lost its w shape through the action of turbulent diffusion. Despite the fact that the thrust measured for the downstream wind turbine was higher for Setup B ($C_T = 0.53$) than for Setup A ($C_T = 0.35$), the velocity deficit recovered faster in the former case. In fact, the downstream turbine induced a much higher level of turbulent kinetic energy when operating at off-design conditions (compare Figs. 6b to 7b). This increases the recovery rate compared to the optimum wake operation case. The model from Acona still predicted too low velocity at the wake centre line. The actuator disc models from CMR and GexCon, which proved to be quite diffusive, perform well here, predicting a smooth wake shape. Both the LES models from Meventus and Leonardi again fail to predict the velocity deficit at the centre line due to the missing tower and nacelle. Still the latter overestimated the wake width by only 6%, see Table 3. Even though five out of the eight models predicted the wake width within ±15%, the results from the LES by DTU-KTH had the best agreement, closely following the experimental results all across the wake.

The turbulence stress measurements at $X = 1D$ (Fig. 7b) exhibit two primary peaks of different magnitude at $Z = \pm R$, even though the relative difference between their values is only half of what was found for Setup A. The centre of the wake was characterized by a high turbulence level, 50% higher than in Setup A, caused by the additional shear layers induced in the wake by the inner part of the rotor working as propeller. The model from Acona again predicted very low turbulent energy levels, being typically 5 times lower than the measurements. The actuator disc models from GexCon and CMR seem to match the experimental turbulent stresses in the shear layer well, even though the calculations by CMR produced too high turbulence in the wake centre, as it did for Setup A (Fig. 6b). The LES predictions from DTU-KTH overestimated the turbulent stresses all across the wake roughly by a factor of 2. Meventus performed very well in the tip region but poorly near the centre line, where it predicted virtually no turbulence.

Further downstream, at $X = 4D$ (Fig. 7d), the experimental turbulent profile is characterized by the two peaks, very similar in magnitude and shape to those observed for Setup A (Fig. 7). The distinct turbulence peaks predicted at $X = 1D$ by CMR and the GexCon models have diffused too fast, and are now less than half the measured levels, as it was also observed for Setup A. The $k-\omega$ SST model from Acona gives the lowest predictions, basically

maintaining the same level of turbulence calculated for $X = 1D$. On the other hand, the LES results from Meventus feature extreme turbulent energy levels at $Z = \pm R$, being almost twice as high as at the upstream position and twice as high as the measured values. As can be seen from the mean velocity profiles, the model is underestimating turbulent cross-stream diffusion, which means that steep gradients can persist also far from the turbine rotor and give birth to considerable production of turbulent stresses. The LES from DTU-KTH agrees well with the measurements, matching the maximum turbulent stress values. This also applies to the RSM actuator disc from De Vaal, which shows very good agreement except at the centre of the wake, where turbulence production is overestimated due to the presence of two additional shear layers. In Table 4, it may be seen that seven out of eight models underestimated the centerline normal stress, but all of the predictions but Acona correctly predicted at least the order of magnitude of the centerline and maximum normal stresses.

The challenges for this off design condition were represented by the mixed working conditions of the rotor. The LES from DTU-KTH initially produced very high levels of turbulence, but managed to reproduce the dynamics of the wake and therefore quickly produced a turbulent stress profile in close agreement with the measurements. Again, modelers who have been using a 2-equation turbulence closure failed to correctly represent the evolution of the turbulent stresses.

3.2.3. Setup C ($\lambda_1 = 6, \lambda_2 = 2.5$)

In Setup C the downstream turbine produced 67% of its peak energy output when operating in the wake of T1. As mentioned in section 3.1, due to the low tip speed ratio, the inner sections of the rotor are stalled, while the outer sections are operating at relatively high angles of attack. In Fig. 8a, the wake is characterized by a lower average velocity than setup A, the thrust being lower by a factor of 4, but the velocity profile is more uniform.

The Acona model, which has performed well in the near wake for the other two Setups, here underestimates the centerline wake velocity by 20%, but is accurate in reproducing the wake width. This is probably due to a prediction of the stall of the inner rotor sections that is not sufficiently severe. As a consequence the thrust is overestimated, see Fig. 5. The simulation from CMR matches the profile closely, especially close to the centerline. The LES from Meventus and the RANS from GexCon-sim2 underestimate the velocity outside of the wake by about 20%. The simulation from DeVaal shows a very good match here, despite an even lower predicted thrust. This can be explained by the thick boundary layer on the wind tunnel walls simulated by DeVaal, visible at $Z = \pm 3R$ in Fig. 8a, which creates additional blockage. Among the three LES simulations that used the actuator line model, the DTU-KTH performs best near the centre of the wake, but the calculated wake width is too small despite the perfect thrust prediction. In this setup the tower and nacelle thrust accounts for 30% of the rotor thrust. The support structure thrust has been subtracted from the thrust measurement shown in Fig. 4, but its effect modifies the velocity profiles, especially when the rotor thrust is low. Therefore, even when the rotor thrust is correctly predicted, not including the nacelle and the hub in the simulation can never faithfully reproduce the wake development.

Further downstream, (Fig. 8c), the experimental maximum velocity deficit is roughly the same as for the upstream station ($U/U_{ref} \approx 0.5$). However, diffusion has smoothed the velocity gradients, giving the profile a more Gaussian shape. Here six out of eight simulations agree to within 15% about the wake width, see also Table 3, while there is more scatter with respect to the centre line velocity value. The actuator disc simulation from CMR is the most accurate, reproducing the measurements well, while the two simulations from GexCon only partly reproduce the wake. GexCon-sim1 fails by 25% near the centre, but performs very well in the outer part, while the opposite applies to GexCon-sim2. The LES from Leonardi and Meventus feature a strong mean velocity peak at the centre line, caused by the flow bypassing the rotor where the nacelle should be, while in DTU-KTH model turbulent diffusion has already almost completely smeared out this peak.

The turbulence in the shear layer measured at $X = 1D$ for this case is lower than for the other two setups, being almost 1.5 times smaller than for setup A (Fig. 8b). The low rotor thrust induced lower mean velocity gradients and as a consequence lower turbulence production in the shear layer. The profile features three peaks, two in the shear layer and one downstream of the nacelle and tower, the latter being slightly offset toward the positive Z axis due to the wake rotation. The simulations reproduce the same general behavior observed in the other cases; the 2-equation turbulence closure models estimate too low turbulence production in the shear layer and were not able to pick up the asymmetries in the flow. The RSM simulation from DeVaal overpredicts the turbulent stress in the left shear layer roughly by a factor 2. Only the DTU-KTH simulation predicts a significant amount of turbulent energy at the rotor centerline, but the level is much too high all across the wake. At $X = 4D$ (Fig. 8d), the LES of DTU-KTH closely matches the experimental profile along the negative Z axis, but produced an asymmetric profile that predicts too low energy level on the opposite side. There is nothing in this simulation that should generate an asymmetry, so this could indicate that the sampling time may have been to short. The turbulent normal stresses predicted by the actuator disc models from GexCon and CMR is, as for the previous measurement station, too low by a factor of 2 and 4, respectively (see Table 4).

The results from Setup C allows us to draw some interesting conclusions. Firstly, the fully resolved simulation from Acona, which had performed so well in the near wake for the first setups, showed some limitations in predicting the stall on the inner rotor sections of the downstream turbine. Secondly, the low turbulence content in the wake in Setup C seemed to create more challenges to the predictions than the other more turbulent cases. At $X = 4D$ the agreement amongst the different models on the velocity profiles was very poor, especially near the rotor tip area, where the predicted turbulence kinetic energy level varied almost by an order of magnitude.

3.2.4. Setup A: vertical diagonal

So far only data along the horizontal diagonals have been presented. For all test cases and all stations measurements and predictions were available both along a horizontal and vertical diagonal through the centre of the wake. In the physical space the flows along these two lines are quite different, since there are no symmetry lines (see Fig. 1). Since most of the predictions incorporated some form of symmetry boundary conditions, these methods will produce identical results along the two lines. Therefore only vertical profiles for one test case will be presented here for the benefit of the methods that included all the details of the model turbines.

The measured vertical profile of the mean velocity at $X = 1D$ for Setup A is shown in Fig. 9a. It may be seen to be markedly different from the profile along the horizontal diagonal that was shown in Fig. 6a. The height of the wind tunnel is $Y \approx \pm 2R$, with the model centre line being 0.1R below the tunnel centre line. Hence, considering also the presence of the turbine tower, there will be a higher solid blockage effect on the lower side of the wake ($\sigma_l = 18.9\%$) than on the upper side ($\sigma_u = 10.5\%$). Neither of these effects are included in prediction models that rely on symmetry. Fig. 9a clearly shows the asymmetry in the measurements where the velocity on the negative Y side is seen not to recover to the free

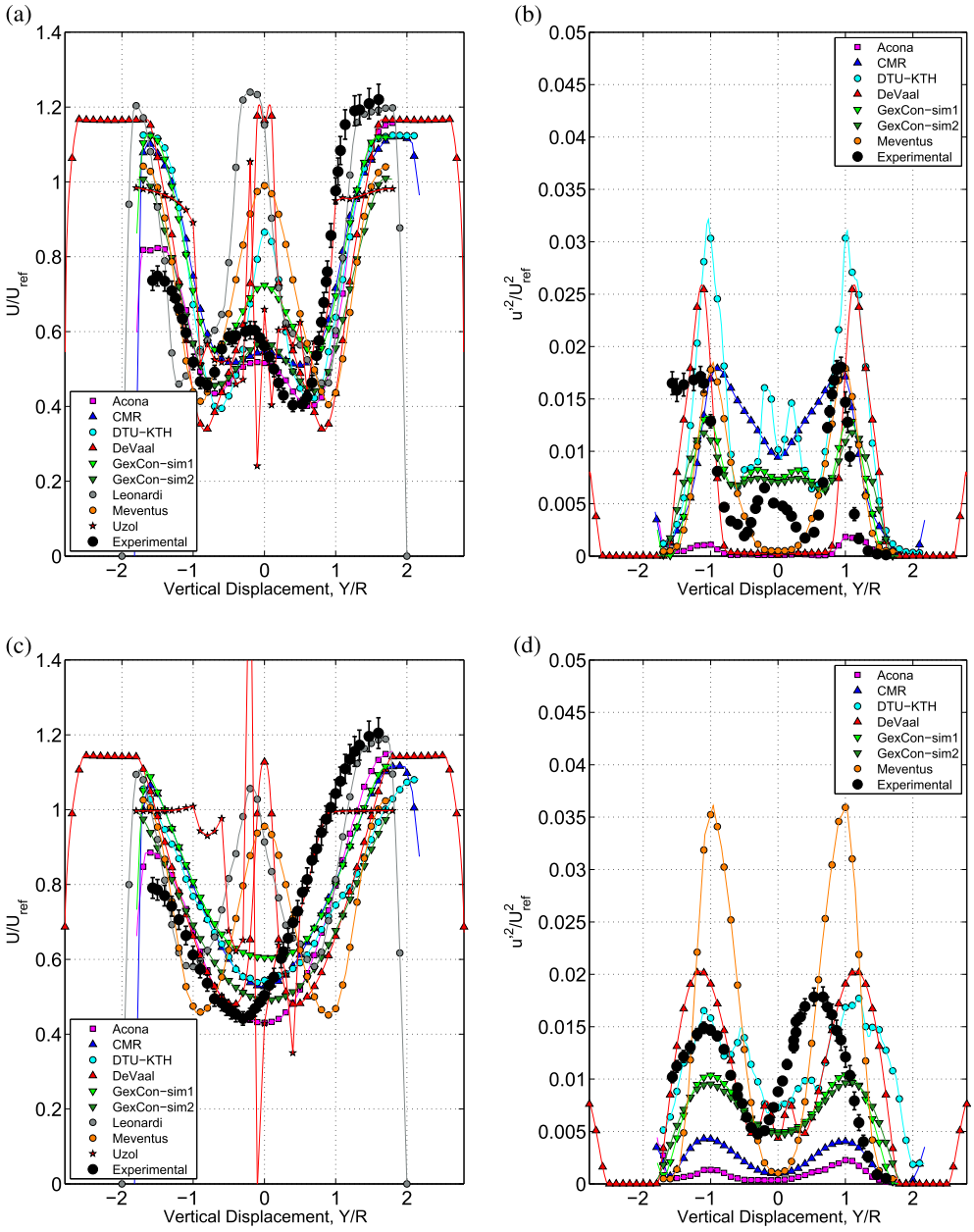

Fig. 9. Wake predictions for the turbine tandem, Setup A, along a vertical diagonal. The upstream turbine was running at $\lambda_1 = 6$ while the downstream turbine at $\lambda_2 = 4$. (a): U/U_{ref} at $X = 1$D, Vertical, Setup A. (b): u'^2/U^2_{ref} at $X = 1$D, Vertical, Setup A. (c): U/U_{ref} at $X = 4$D, Vertical, Setup A. (d): u'^2/U^2_{ref} at $X = 4$D, Vertical, Setup A.

stream velocity. In addition, the maximum velocity deficits above and below the wake centre line are different.

The simulations by Acona included the tower and tunnel geometry. It therefore reproduced this asymmetry and match the velocity profile along the negative Y axis quite well. CMR included the effect of the hub but not of the tower, hence their profiles are also symmetric. The methods who have not included the hub experienced particularly high values of the velocity at $Y = 0$, consistent with the horizontal case. From the hot wire measurements it is also possible to observe a distinct downward shift of the whole wake structure. This effect has been found to be connected to the presence of the turbine tower wake which pulls the rotor wake structure towards the floor.

The methods from Acona, Meventus and DTU-KTH matched the maximum velocity deficit of the positive Y axis. Meventus and DTU-KTH included the tunnel walls in their simulations, but only the Acona simulation included the tower and the nacelle and therefore was the only one that managed to reproduce the asymmetry in the velocity profile.

Further downstream, at $X = 4$D (Fig. 6e), the measured mean velocity profile is significantly smoother than for the upstream position, but with strong asymmetry. The wake is clearly seen to be shifted down towards the floor. No method seems to catch this behavior. Furthermore, there appears to be a strong disagreement between the models about the wake width, which seems to be generally overestimated.

The measured normal stress, shown in Fig. 9b, clearly includes the stress produced by the tower wake. Further downstream (Fig. 6f) the turbulent stress peaks are as strong as at $X = 1$D, although not as sharp, indicating both important turbulence

production and diffusion between the two stations. The DTU-KTH and the De Vaal models show good agreement with the maximum stresses from the experiments. The observations about the different models that were made for the horizontal profiles hold also for the vertical ones, and in particular that models using 2-equation closure techniques seem to underestimate the turbulence stress magnitude. The predictions by Acona reproduce the asymmetry of the measured profile, but the level is again much too low.

4. Conclusions

The work here reported is the result of a "blind test" challenge consisting of two wind turbines operating in-line with a downstream separation of 3D. Modelers were invited to predict the performance of the turbines as well as the wake developments, only knowing the wind tunnel boundary conditions and the geometry of the two model turbine located in a large scale wind tunnel. This is typical of the engineering task when e.g. designing a wind farm, where no result are known a priori. Hence the skill of the model operator becomes important, both in setting up the simulation, in choosing the optimal model parameters and in analyzing the validity of the simulation result.

At the workshop, experimental data were presented by the organizers and compared with the simulations submitted by eight research groups, who produced nine different numerical predictions. Three contributions used LES models coupled with an actuator line model of the rotor, three RANS simulations using actuator disc model of the rotor were received, one U-RANS simulation with fully resolved turbine geometry was presented and finally results from a vortex panel code was submitted.

The comparisons between simulations and the experimental data showed that the modeling of the upstream turbine working in uniform, low turbulence flow at optimum performance which was the topic also for the first blind test organized (documented in Krogstad and Eriksen [17]), despite being the most basic of the test cases, still represented a challenge. The scatter between the power generation predicted by the models was considerable ($\pm$20%), and even larger for the thrust, where the variation between the predictions was as much as 75% of the experimental value. The Acona model, which fully resolved the rotor and turbine geometry, gave the best estimates both for power and thrust. The only other model that fully resolved the blade surface via vortex panel method, did not give reliable predictions for the upstream turbine, maybe due to a too short sampling time. The scatter between the simulations making use of a Blade Element Momentum (BEM) rotor model was larger than expected. This can partly be traced back to the uncertainties in the airfoil lift and drag performance data that the participants had to generate themselves. However, even when two BEM models used the same 2D airfoil data, the output turned out to be quite different, as in the case of the RANS actuator disc from deVaal and the LES actuator line model from DTU-KTH. As already observed in previous blind tests, simulations giving very wrong power productions could still generate good thrust prediction, and vice versa, depending on the estimated lift and drag coefficients as function of the angle of attack.

For a correct prediction of the downstream turbine power output, the computational model needs to faithfully reproduce the wake of the upstream turbine and be capable of handling its effects on stall and off-design working conditions for the downstream rotor. Therefore the fully resolved Acona model gave the best overall agreement with the experimental power and thrust coefficients, both when the downstream turbine was operated at low and high tip speed ratios. At $\lambda_2 = 2.5$, the results from the BEM models were mostly acceptable, probably due to good predictions of the post stall characteristics of the airfoil. The rather high power output predictions for the downstream turbine from DeVaal can be traced back to a higher wake recovery rate predicted by his RANS simulation. The largest scatter between the models was observed at the high tip speed ratio near the runaway point. Only three out of eight models managed to reproduce a close to zero power production here. Hence the tip speed at the runaway point would have been seriously overestimated by most models leading to considerable over-predictions of maximum blade loads. At $\lambda_2 = 4$, all the LES simulations overestimated the downstream turbine power production, consistent with the underprediction of the upstream turbine thrust. The efficiency predicted by the RANS computations, on the other hand, were equally scattered around the experimental value ($\pm$50%). This indicates that the LES predictions are on average more accurate than the RANS computation. The rather tight spacing between the turbines gave a distinct advantage to models which reproduced the near field of the upstream turbine wake well.

Close to the rotor, where the wake directly reflects the aerodynamic performance of the rotor, the Acona model performed the best, perfectly matching the measurements in setup B. On the other hand, the predicted turbulent kinetic energy was much too low in all the test cases. This limited the effects of turbulent diffusion on the mean velocity profiles and reduced the accuracy of the wake predictions further from the turbine. Some models, like the DTU-KTH actuator line, despite outputting inaccurate thrust values for the rotor, managed to reproduce the turbulent stress magnitude even at a short distance from the turbine and therefore to accurately predict the wake far from the rotor.

Also the LES simulation from Meventus produced reliable turbulence levels in near wake shear layer. However, the mean velocity and turbulent energy profiles showed very little sign of diffusion while evolving downstream, which seems unphysical also in the light of the coarse computational mesh used, which is expected to introduce a substantial amount of numerical diffusion.

The RANS models that used 2-equation turbulence closure approximations generally underestimated the turbulent stress magnitude and overestimated its dissipation rate, probably due to the anisotropy of the turbulent stresses. The RANS computation from DeVaal, using a Reynolds stress (RSM) turbulence closure model and incorporating an axisymmetry simplification, generated better turbulent stress predictions than the 3D simulation from GexCon.

Along a vertical diagonal, most of the models predicted the same results as for the horizontal diagonal, while measurements showed distinct differences caused by the wake from the tower, especially in the mean velocity profiles. This was not picked up by most of the simulations primarily because many of the models had incorporated symmetry approximations in order to reduce the computational efforts. The measurements showed a tendency for the wake to move down towards the ground as it evolves downstream, a trend that was not picked up in any of the simulations.

The blind test exercise, despite giving very good indications on the performance of various turbine models, has some limitations. To achieve a more direct comparison of models making use of a BEM approach for the rotor modeling, it would probably have been better to provide all the participants with a well defined set of 2D airfoil data for all to use in order to remove one possible source of uncertainty. The two main parameters influencing the outcome of the simulations were without doubt the modeling of the forces from the rotor onto the flow and the turbulent transport models applied in the wake. If these are not correctly handled, it will strongly affect the inflow to the second turbine, affecting the predicted performance. As a consequence the predictions of the characteristics of the second wake, which was the main attention of this blind test, was severely affected. Some indications of this

problem is evident in the performance characteristics predicted for the second turbine, but unfortunately documentation of the inflow to the second turbine was not requested by the organizers. As for the test case geometry, the influence of the turbine towers is not negligible and it created much greater differences between the horizontal and vertical profiles than what could be expected in a full scale case, because the tower to rotor diameter is exaggerated. However, the wind turbine models were specifically designed as a test case for modelers and not meant to directly mimic a particular full scale turbine. Therefore the differences between the simulations and the experiment simply point out that the tower and nacelle geometries should not be ignored in the simulations.

The results of this blind test show that predicting the performance of two turbines operating in-line is a considerable challenge and that none of the models applied here have reached the necessary maturity to be used indiscriminately for the design of wind farms. The fully resolved simulation proved to be quite reliable when it comes to predicting turbine performances and gave the best agreement with the measurements on power and thrust coefficients over the tip speed range investigated here. However, its prediction of turbulent kinetic energy in the wake was less impressive, suggesting that dynamic loads on a downstream turbine may be severely under-predicted. Estimating correct turbulent momentum transport has proven to be a key issue for getting the velocity recovery rate in the wake correct and from the current comparisons it seems that a LES method coupled with an actuator line model is at present the best option.

References

[1] Adaramola MS, Krogstad P-Å. Experimental investigation of wake effects on wind turbine performance. Renew Energy 2011;36:2078–86.
[2] Ainslie J. Calculating the flowfield in the wake of wind turbines. J Wind Eng Indus Aerodyn 1988;27:213–24.
[3] Alfredsson P, Dahlberg JÅ. Measurements of wake interaction effects on the power output from small wind turbine modelsIn The Aeron. Int. of Sweden, vol. 82; 1981. Technical Note HU-2189.
[4] Chamorro L, Porté-Agel F. A wind-tunnel investigation of wind-turbine wakes: boundary-layer turbulence effects. Bound Layer Meteor 2009;132:129–49.
[5] Churchfield M, Lee S. Ntwc - simulator for offshore wind farm applications (sowfa). Website, http://wind.nrel.gov/designcodes/simulators/sowfa/; 2012.
[6] Crespo A, Hernández J, Fraga E, Andreu C. Experimental validation of the UPM computer code to calculate wind turbine wakes and comparison with other models. J Wind Eng Indus Aerodyn 1988;27:77–88.
[7] Delany N, Sørensen N. Low-speed drag of cylinders of various shapes. Technical Report 3038. National Advisory Committee for Aeronautics; 1953.
[8] Drela M. XFOIL: an Analysis and Design System for Low Reynolds Number Airfoils. Technical Report, NREL; 1989.
[9] Ferziger JH, Perić M. Computational methods for Fluid Dynamics, volume 3. 2nd ed. 2001.
[10] García NR. Unsteady viscous-Inviscid Interaction Technique for Wind Turbine Airfoils. DTU; 2011. Ph.D. thesis.
[11] Grant I, Parkin P, Wang X. Optical vortex tracking studies of a horizontal axis wind turbine in yaw using laser-sheet flow visualisation. Exp Fluids 1997;23:513–9.
[12] Hansen C. Nwtc - an excel workbook for generating airfoil tables for aerodyn and wtperf(airfoilprep). Website, https://wind.nrel.gov/designcodes/preprocessors/airfoilprep/; 2012.
[13] Hansen M. Aerodynamics of wind turbines. 2nd ed. Earthscan; 2008.
[14] Jensen NO. A note on wind generator interaction. RISØ; 1983.
[15] Krogstad P-Å, Adaramola MS. Performance and near wake measurements of a model horizontal axis wind turbine. Wind Energy 2012;15:743–56.
[16] Krogstad P-Å, Eriksen PE. "Blind Test" Workshop. Technical Report. NTNU; 2011.
[17] Krogstad P-Å, Eriksen PE. "Blind test" calculations of the performance and wake development for a model wind turbine. Renew Energy 2013;50:325–33.
[18] Krogstad P-Å, Lund JA. An experimental and numerical study of the performance of a model turbine. Wind Energy 2011;15:443–57.
[19] Launder B, Spalding D. The numerical computation of turbulent flows. Comput Meth Appl Mech Eng 1974;3:269–89.
[20] Maeda T, Yokota T, Shimizu Y, Adachi K. Wind tunnel study of the interaction between two horizontal axis wind turbines. Wind Eng 2004;28:197–212.
[21] Mann J. Wind field simulation. Probabilist Eng Mech 1998;13:269–82.
[22] Medici D, Alfredsson P. Measurements on a wind turbine wake: 3D effects and bluff body vortex shedding. Wind Energy 2006;9:219–36.
[23] Pierella F, Eriksen PE, Sætran L, Krogstad P-Å. Invitation to the 2012 "Blind test 2" workshop - calculations for two wind turbines in line. Invitation. Norwegian University of Science and Technology - NTNU; 2012.
[24] Pope S. Turbulent Flows. Cambridge University Press; 2000.
[25] Sagaut P. Large eddy simulation for incompressible flows. Springer; 2006.
[26] Sarmast S. Numerical study on instability and interaction of wind turbine wakes. Licentiate thesis. Stockholm: KTH; 2013.
[27] Schümann H, Pierella F, Sætran L. Experimental investigation of wind turbine wakes in the wind tunnel. Energy Procedia 2013;35:285–96. DeepWind 2013 Selected papers from 10th Deep Sea Offshore Wind Conference, Trondheim, Norway, 24–25 January 2013.
[28] Sha W, Launder B. A model for turbulent momentum and heat transport in large rod bundles. Technical Report 73, Argonne Lab. Rep. AN-77; 1979.
[29] Simms D, Schreck S, Hand M, Fingersh L. NREL unsteady aerodynamics Experiment in the NASA-Ames wind tunnel: a comparison of predictions to measurements. Technical Report. NREL; 2001.
[30] Smith D. Multiple wake measurements and analysis. In: Davies T, Halliday J, Palutikov J, editors. Proceedings of the 12th BWEA Wind Energy; 1990. pp. 53–8.
[31] H. Snel H, J. Schepers J, B. Montgomerie B,. The Mexico project (model experiments in controlled conditions): the database and first results of data processing and interpretation,. In: Journal of Physics: Conference Series, vol. 75, IOP Publishing, p. 12-14.
[32] Somers D. Design and experimental results for the S825 Airfoil. Technical Report NREL/SR-500-36344. National Renewable Energy Laboratory; 1999.
[33] Sørensen JN, Shen WZ, Munduate X. Analysis of wake states by a full-field actuator disc model. Wind Energy 1998;1:73–88.
[34] Tangler JL, Somers DM. NREL airfoil families for HAWTs. In: Proceedings of the American Wind Energy Association Windpower Conference. Washington: National Renewable Energy Laboratory; 1995.
[35] Troldborg N. Actuator line simulation of wake of wind turbine operating in turbulent inflow. In: EWEC 2009, vol. 75. IOP Publishing; 2007. pp. 20–63.
[36] Vermeer LJ, Sørensen JN, Crespo A. Wind turbine wake aerodynamics. Prog Aerosp Sci 2003;39:467–510.
[37] Wood D. Some effects of compressibility on horizontal-axis wind turbines. Renew Energy 1997;10:11–7.
[38] Zahle F, Sørensen NN, Johansen J. Wind turbine rotor-tower interaction using an incompressible overset grid method. Wind Energy 2009;12:594–619.